Cell Tissue Bank (2024) 25:255–267
https://doi.org/10.1007/s10561-021-09976-y

Effects of mesenchymal stem cell culture on radio sterilized human amnion or radio sterilized pig skin in burn wound healing

B. Cabello-Arista · Y. Melgarejo-Ramírez · A. Retana-Flores · V. Martínez-López · E. Márquez-Gutiérrez · J. Almanza-Pérez · H. Lecona · M. L. Reyes-Frías · C. Ibarra · M. E. Martínez-Pardo · C. Velasquillo · R. Sánchez-Sánchez

Received: 17 April 2020 / Accepted: 2 November 2021 / Published online: 20 January 2022

Abstract Deep second and third degree burns treatment requires fibroblasts, keratinocytes and other skin cells in order to grow new dermis and epidermis. Cells can proliferate, secrete growth factors and extracellular matrix required to repair the damaged tissue. Radiosterilized human amnion and radiosterilized pig skin have been used as natural origin skin dressings for burned patients. Adipose-derived mesenchymal stem cells can differentiate into fibroblasts and keratinocytes and improve wound-healing progress. These cells can stimulate vascular tissue formation, release growth factors, synthetize new extracellular matrix and immunoregulate other cells. In this study, we developed mesenchymal stem cells-cellularized skin substitutes based from radiosterilized human amnion or pig skin. Third-degree burns were induced in mice animal models to evaluate the effect of cellularized skin substitutes on burn wound healing. Mesenchymal phenotype was immunophenotypically confirmed by flow cytometry and cell viability was close to 100%. Skin recovery was evaluated in burned mice after seven and fourteen days post-coverage with cellularized and non-cellularized sustitutes. Histological techniques and immunofluorescence were used to evaluate re-epithelization and type I collagen deposition. We determined that cellularized-human amnion

B. Cabello-Arista and Y. Melgarejo-Ramírez have contributed equally to this work.

Supplementary Information The online version contains supplementary material available at https://doi.org/10.1007/s10561-021-09976-y.

B. Cabello-Arista · Y. Melgarejo-Ramírez · E. Márquez-Gutiérrez · C. Velasquillo
Laboratorio de Biotecnología, Instituto Nacional de Rehabilitación Luis Guillermo Ibarra Ibarra, Calzada México-Xochimilco No. 289, Col. Arenal de Guadalupe, C.P. 14389 Mexico City, Mexico

A. Retana-Flores · V. Martínez-López · C. Ibarra · R. Sánchez-Sánchez (✉)
Unidad de Ingeniería de Tejidos, Terapia Celular y Medicina Regenerativa, Instituto Nacional de Rehabilitación Luis Guillermo Ibarra Ibarra, Calzada México-Xochimilco No. 289, Col. Arenal de Guadalupe, C.P. 14389 Mexico City, Mexico
e-mail: robsanchez@inr.gob.mx; sanchez2.roberto@gmail.com

J. Almanza-Pérez
Laboratorio de Farmacología, Depto. Ciencias de la Salud, D.C.B.S.,, Universidad Autónoma Metropolitana-Iztapalapa, C.P. 09340 Mexico City, Mexico

H. Lecona
Bioterio y Cirugía Experimental, Instituto Nacional de Rehabilitación Luis Guillermo Ibarra Ibarra, Calzada México-Xochimilco No. 289, Col. Arenal de Guadalupe, C.P. 14389 Mexico City, Mexico

M. L. Reyes-Frías · M. E. Martínez-Pardo
Banco de Tejidos Radioesterilizados, Instituto Nacional de Investigaciones Nucleares (BTR-ININ), Carretera México-Toluca S/N La Marquesa, C.P. 52750 Ocoyoacac, Edo. Mex, Mexico

or cellularized-pig skin in combination with mesenchymal stem cells improve extracellular matrix deposition. Both cellularized constructs increase detection of type I collagen in newly formed mouse skin and can be potentially used as skin coverage for further clinical treatment of burned patients.

Keywords Burns · Radiosterilized human amnion · Radiosterilized pig skin · Mesenchymal stem cells · Cellularized-skin substitutes · Type I collagen

Introduction

Burns are one of the most common causes of skin damage. For patients with deep second and third-degree burns, gold standard treatment involves healthy skin autografting. It has been described that, for patients with over 40% of total burn surface area (TBSA), autografting is difficult to perform (Peck 2011). Non-cellularized skin substitutes are one of the most used coverages for the treatment of burned patients; however, treatment of deep burns requires fibroblast and keratinocytes in order to grow new dermis and epidermis. Therefore, cells that proliferate, migrate, secrete growth factors, chemokines and extracellular matrix (ECM) are required to be cultured in a wide variety of biocompatible scaffolds in order to repair the damaged tissue.

Cellularized skin substitutes are the best option for skin coverage when TBSA does not allow use of autografts in burn patients (Kinsner et al. 2001; Llames et al. 2006; Auger et al. 2009). Mesenchymal stem cells (MSC) are multipotent stromal cells able to reduce inflammation, generate vascular tissue, may differentiate into fibroblasts and keratinocytes, and secrete growth factors and ECM involved in wound healing (Fathke 2004; Aggarwal and Pittenger 2005; Wu et al. 2007; Sasaki et al. 2008; Hocking and Gibran 2010). One of the greatest advantages from MSC is that they can be obtained from different sources in adults and added as cellular component in skin substitutes to prevent rejection and disease transmission (Galipeau and Sensébé 2018).

Radiosterilized human amnion (RHA) and radiosterilized pig skin (RPS) are suitable biomaterials for skin coverage due to their ECM components, structure and collagen content. They work as wound dressings not only to prevent infections and water loss, but also as cell carriers to promote tissue recovery. Collagen is the most abundant protein in dermis and it is also the most common used to develop skin substitutes (Jones et al. 2002; Böttcher-Haberzeth et al. 2010; Yildirimer et al. 2012). The aim of this study was to analyze whether radiosterilized human amnion (RHA) or radiosterilized pig skin (RPS) in combination with adipose-derived mesenchymal stem cells improves wound-healing progress in a deep-burn animal model.

Materials and methods

Biological scaffolds

Radiosterilized human amnion (RHA) and radiosterilized pig skin (RPS) were processed and supplied from *Banco de Tejidos Radioesterilizados* of the *Instituto Nacional de Investigaciones Nucleares* (BTR-ININ). The processing and final radiation sterilization was performed according to standard operation procedures, as requested by the quality management system of ININ that applies to the processing, research and development of biological tissues sterilized with ionizing radiation, as previously described (Martínez-Pardo and Mariano-Magaña 2007; Sánchez-Sánchez et al. 2015). The 25 kGy radiation sterilization dose was calculated following the *Código de Prácticas para la Esterilización por Irradiación de Tejidos Humanos para Uso Clínico: Requisitos para la Validación y Control de Rutina*, OIEA, 2013.

Mesenchymal stem cell isolation and culture

Human adipose tissue (AT) was obtained from aesthetic surgeries under informed consent and transported in 10% penicillin/streptomycin/DMEM-F12 medium (Gibco). Briefly, tissue was washed with phosphate buffered saline (PBS, Gibco) 10% antibiotic for 10 min and digested with 1% Type II collagenase [3 mg/mL] (Worthington Biochemicals)

R. Sánchez-Sánchez
Escuela de Ingeniería y Ciencias, Departamento de Bioingeniería, Instituto Tecnológico de Monterrey, Puente 222, Col. Arboledas del Sur, C.P. 14380 Mexico City, Mexico

during 40 min. The stromal vascular fraction (SVF) was collected and centrifuged at 1200 rpm during 5 min. Cell pellet was resuspended in 10% fetal bovine serum (FBS, Gibco) and 1% of penicillin/streptomycin-supplemented medium. Cells were counted and seeded at 50,000 cell/cm^2 in T25 culture flasks for 24 h. Cells that failed to attach were washed with PBS and new supplemented medium was added.

Cell immunophenotype characterization

To analyze the immunophenotype of ADMSC, a flow cytometry test was carried out using CD90-APC (BD), CD73-APC (BD), CD44-FITC, and CD105-PE as MSC positive markers, and HLA-DR-APC, CD45-FITC (BD), and CD34-PE (BD) as negative markers. Data analysis was performed with the Cell Quest Pro software (Becton Dickinson Immunocytometry Systems).

Generation of constructs and cell viability assay

Mesenchymal stem cells (MSCs) were seeded onto 2.0 cm^2 RHA and RPS pieces at a density of 60,000 cell/cm^2 and incubated for 1 h to allow cells attachment. Biomaterials were then covered with a supplemented medium on 24-well culture plates and incubated at 37 °C, 5% CO_2 during 24 h before implantation. After 24 h, cell viability assay was conducted on cells seeded onto cellularized RHA and RPS constructs, and before implantation. Calcein assay (Live/Dead, viability/cytotoxicity for mammalian cells, Molecular Probes®) was performed following manufacturer's instructions. Briefly, constructs were incubated in 1 μM of calcein AM and 2 μM of EthD-1 solution for 45 min at 37 °C. Constructs were washed with PBS and fluorescent signal was detected using an AxioVision epifluorescence microscope (Carl Zeiss).

Construct implantation in a mouse model of deep burn

The *Instituto Nacional de Rehabilitación Luis Guillermo Ibarra Ibarra* Animal Care Committee (CICUAL) approved all procedures (protocol number 26/13). Three-month old male athymic nude mice (Nu/Nu) were used for a deep-degree burn model. Animals were anesthetized with 5% isoflurane, followed by 1% isoflurane to actually perform the procedure. A circular 2 cm^2 cooper device and a 0.5-kg support were heated to 105 °C for 20 s. The device was then carefully placed on the back of the anesthetized mice for 5 s and quickly removed. Burned area was debrided with a scalpel to remove necrotic tissue. RHA or RPS-MSCs constructs were washed with PBS, placed onto the burned area with the cellular component facing the wound, and covered with hypoallergenic adhesive (Tegaderm). Experimental conditions were as followed: MSC-cellularized RHA (RHA + MSC), MSC-cellularized RPS (RPS + MSC), non-cellularized RHA (RHA), non-cellularized RPS (RPS) and Control (gauze with petroleum jelly). Mice were injected with fentanyl (10 mg/kg) as anesthetic. Photographs of experimental conditions were taken at 7 and 14 days post-burn with a reference scale.

Measurement of wound closure and tissue processing

Five animals were used for each experimental condition, as recommended by the Animal Care Committee. Recovery area during wound closure was measured using photographs taken at the same distance and with a scale located next to the animals. Photographs of wound areas were used to calculate their progression. Histological sections were measured by analyzing the distance between the epithelium of each burn side with the same software. Analysis was performed after 7 and 14 days post-treatment. Animals were euthanized; tissue samples were obtained and fixed in 4% paraformaldehyde for 24 h, dehydrated and paraffin embedded. In order to observe wound healing, 5 μm tissue sections were stained with hematoxylin–eosin, Herovici and Masson's trichrome and examined under light microscopy. Type I collagen (1:100, Abcam) and nuclei (4′,6′-diamidino-2-phenylindole, DAPI) were labeled and examined under epifluorescence microscopy. Images were processed using ImageJ software.

Statistical analysis

For macroscopic photographs, wound size measurement at time zero was considered 100% of the injury. Fluorescence intensity for Type 1 collagen at post-implantation day 7 was calculated in different regions of interest using Image J software. Data from wound closure and collagen fluorescence intensity were

analyzed with Kolgomorov-Smirnov for a normality test. A one-way ANOVA and a Tukey post hoc test were used to compare the sample means.

Results

MSC-cellularized constructs do not promote faster closure of the burned areas.

Adipose-derived mesenchymal stem cells were characterized before construct generation and implantation. Flow cytometry showed positive expression for the characteristic markers, 99.8% CD90, 98.6% CD73, and 97% CD105, and negative expression for hematopoietic markers, including 0.28% CD34, 0.28% CD45 and 0.09% HLA-DR, (Fig. 1). MSC multipotent differentiation, cell viability, adhesion, migration, and cytokines release profile were previously described (Sanchez-Sanchez et al. 2015). Before implantation in deep-burn site, cell viability of MSC in RHA + MSC and RPS + MSC constructs was evaluated to determine whether the cells were alive at the time of treatment or if manipulation had some effects. Calcein assay revealed almost 100% cell viability of MSC at the time they were used to cover deep-degree burn in animal model (Fig. 2a). We confirmed that the hot device used for this study generated a third-degree burn. The temperature calculated with an infrared thermometer was 105 °C, which explained the considerable damage to both, dermis and epidermis (Fig. 2b). Wound closure was analyzed in photographs from each condition. None of the treatments promoted a faster closure of the wound *versus* the control group by post-treatment day 14 (Fig. 3a and b). This result was confirmed analyzing the distance between the opposite sides of the epithelialization zone. Again, no differences were found in wound closure between the control and the experimental conditions on post-treatment days 7 and 14 (Fig. 3c and d).

MSC-cellularized RPS reduced granulation tissue enhanced by RPS itself.

To analyze the histological structure of the skin after treatments with RHA + MSC or RPS + MSC constructs, histological sections were stained with hematoxylin and eosin. By day 7, epithelial layer had not appeared yet covering the wound in any of the treatments, nor the untreated burn *versus* healthy skin (Fig. 4). This is attributable to the third-degree burn, since all the necrotized tissue was removed with a scalpel. Wounds treated with gauze and petroleum jelly (Control) developed some granulation tissue (three arrows), they lost collagen fibers in dermal layer and tissue resembled a homogeneous extracellular matrix (ECM). None of the mice treated with non-cellularized RHA showed a significant development of granulation tissue; however, mice treated with

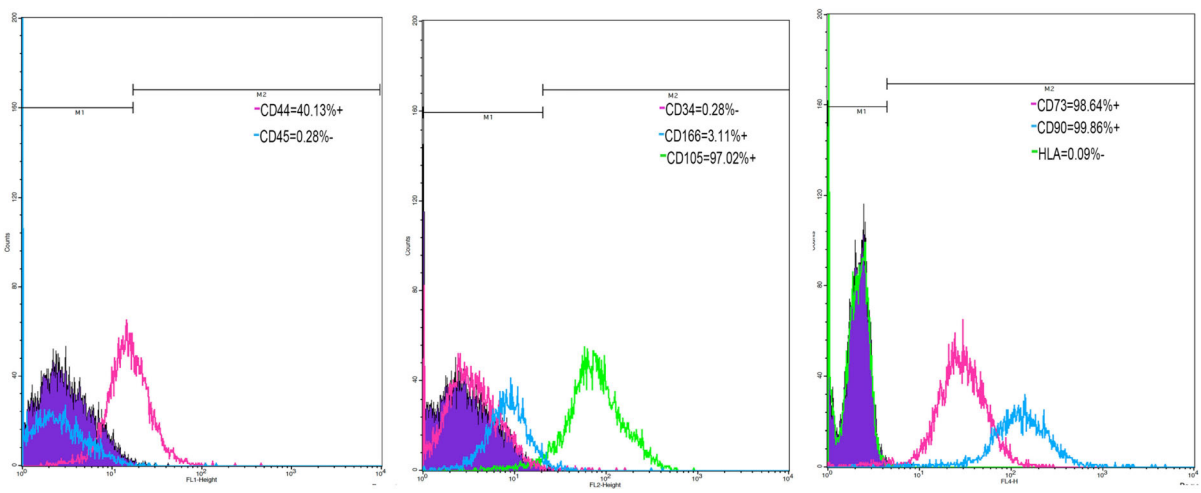

Fig. 1 Immunophenotypic characterization of MSC. Histograms show that mesenchymal stem cells were CD90, CD73, and CD105 positive, but CD34, CD45, and HLA-DR negative

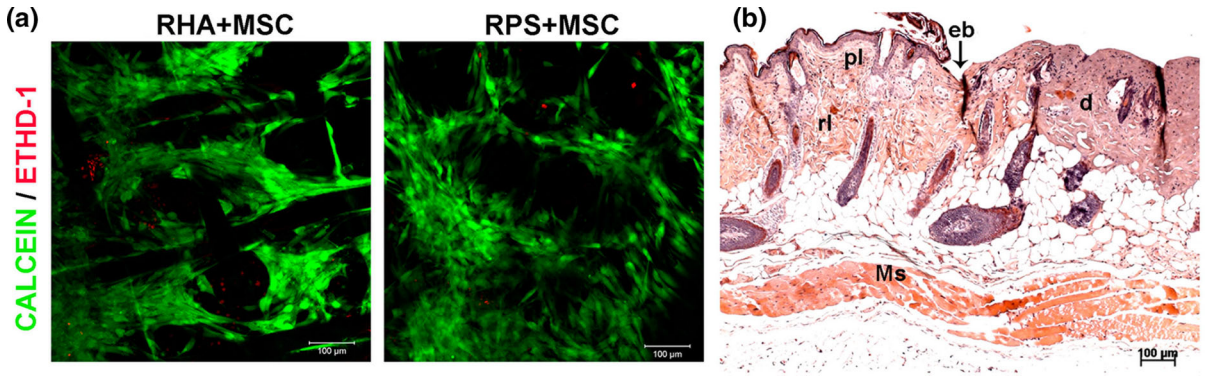

Fig. 2 Cell viability before implantation and histological burn at time 0. **a** Cell viability of mesenchymal stem cells seeded on the radiosterilized pig skin or radiosterilized human amnion. Live cells are stained with calcein (green), while dead cells are ethidium homodimer positive (red). **b** Histological section of mouse skin immediately after the burn (time 0); the edge of the burn (eb) is also visible: to the left, the skin is healthy and there is epidermis; the two dermis layers are also visible: papillary layer (pl) and reticular layer (rl); well organized muscles (Ms) are also visible. To the right of the burn edge, the dermis and the papillary layer are absent; both the reticular layer and muscle section are denatured (d)

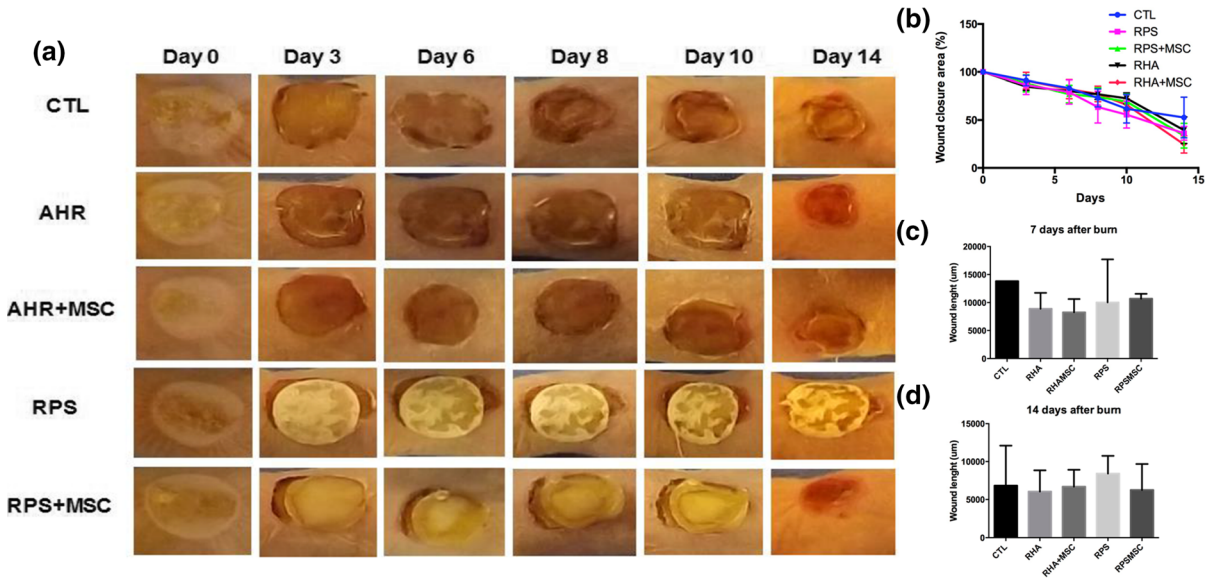

Fig. 3 Constructs fail to enhance wound closure time. **A** Photographs at different days after treatment with all experimental conditions. **B** Percentage of wound closure in all experimental conditions at different days. **C** Distance between new epithelium measured in histological samples at day 7. **D** Distance between new epithelium in histologic samples at day 14

RHA + MSC revealed an increase of granulation tissue was observed. Wounds treated with non-cellularized RPS showed increased granulation tissue but the addition of MSC reduced the presence of granulation tissue. By day 14, all treatments showed basal granulation tissue, which was not significant when compared to day 7 post-implantation (Supplementary Fig. 1).

MSC-cellularized RHA or RPS improves extracellular matrix deposition in deep-burn wound healing.

Different strategies were used to determine if conventional wound dressings or MSC-cellularized constructs regulate extracellular matrix deposition in deep burn wounds. First, Masson's stain was

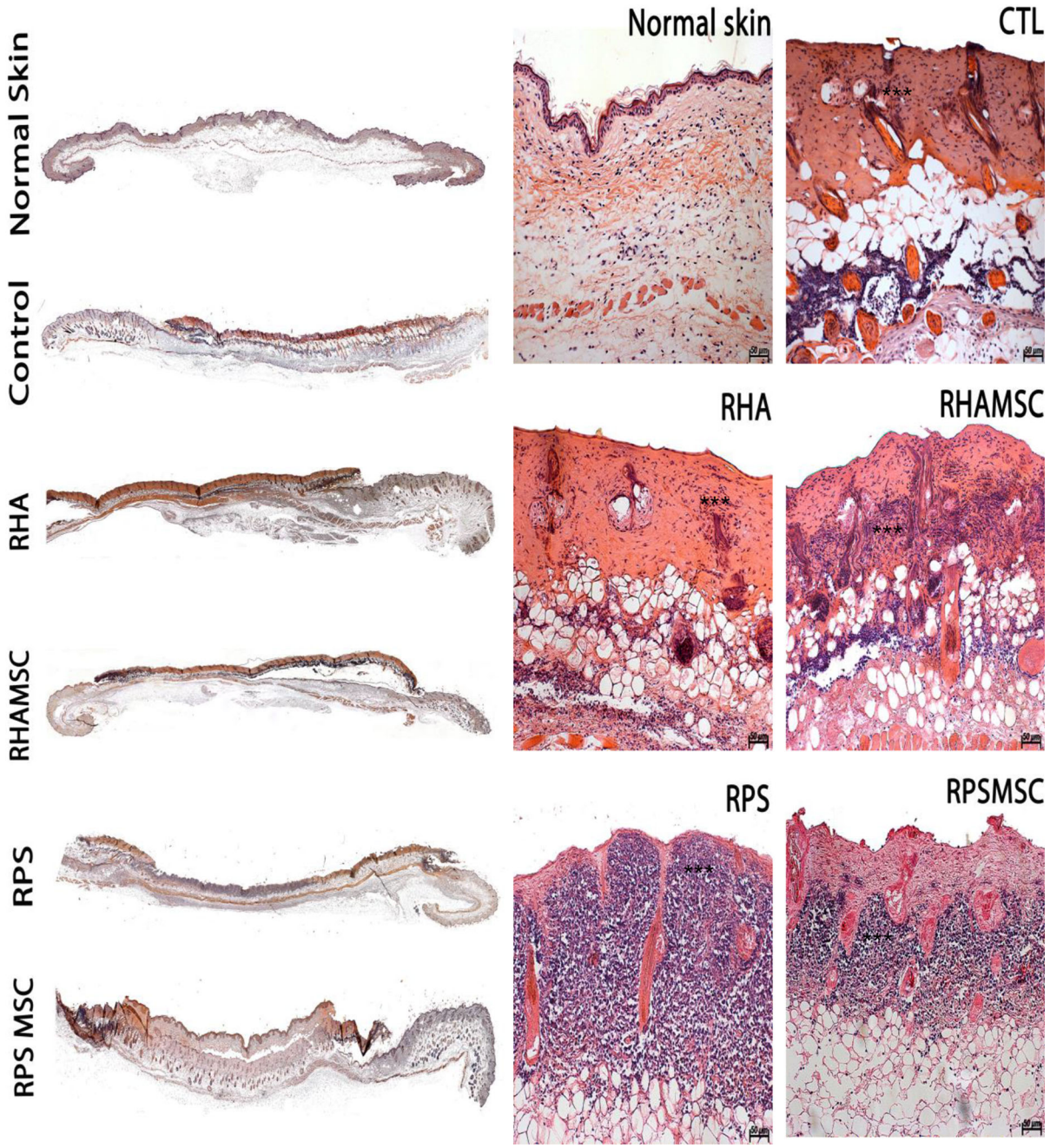

Fig. 4 Granulation tissue increased with RPS treatment, but decreased when in combination with MSC at treatment day 7. Photographs show histological samples stained with hematoxylin & eosin at post-treatment day 7. The images to the left are reconstructions of complete tissue. To the right, three asterisks in the enlarged representative images show a population of granulation tissue. Scale bars represent 50 μm

performed to analyze total collagen deposition after different treatments. In non-wounded skin, most of the ECM found in dermis is constituted by collagen, stained in blue, and epithelium stained in red. On post-burn day 7, control wound treated with petroleum jelly did not show presence of collagen in the dermis, unlike treatments with RHA and RPS, which showed few signs of collagen. However, treatments with RHA +

MSC and RPS + MSC stained positive for collagen deposition, suggesting that MSC-cellularization and RPS improve ECM composition at the same time they protect wound areas (Fig. 5). By day 14-post implantation, all treatments showed presence of collagen, including the control treated with conventional wound dressing, which lacked this characteristic on day 7. Nevertheless, the most intense staining among experimental groups was observed in wounds treated with MSC-cellularized RHA (Fig. 6).

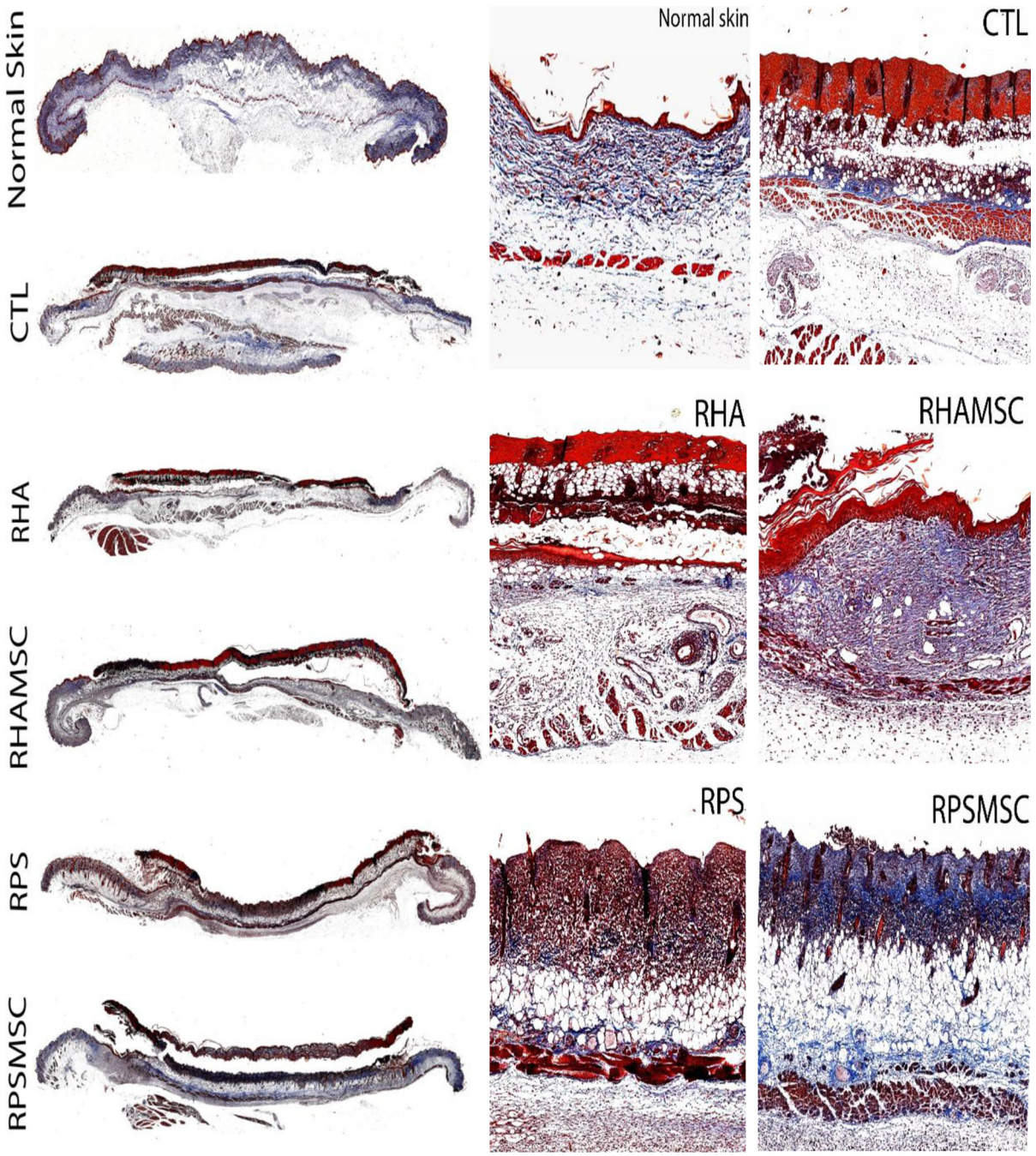

Fig. 5 Collagen deposition is enhanced by constructs. Masson's stain at post-burn day 7. The images to the left are complete reconstructions of the tissues, whereas those to the right are enlarged images of the tissues. Scale bars represent 50 μm

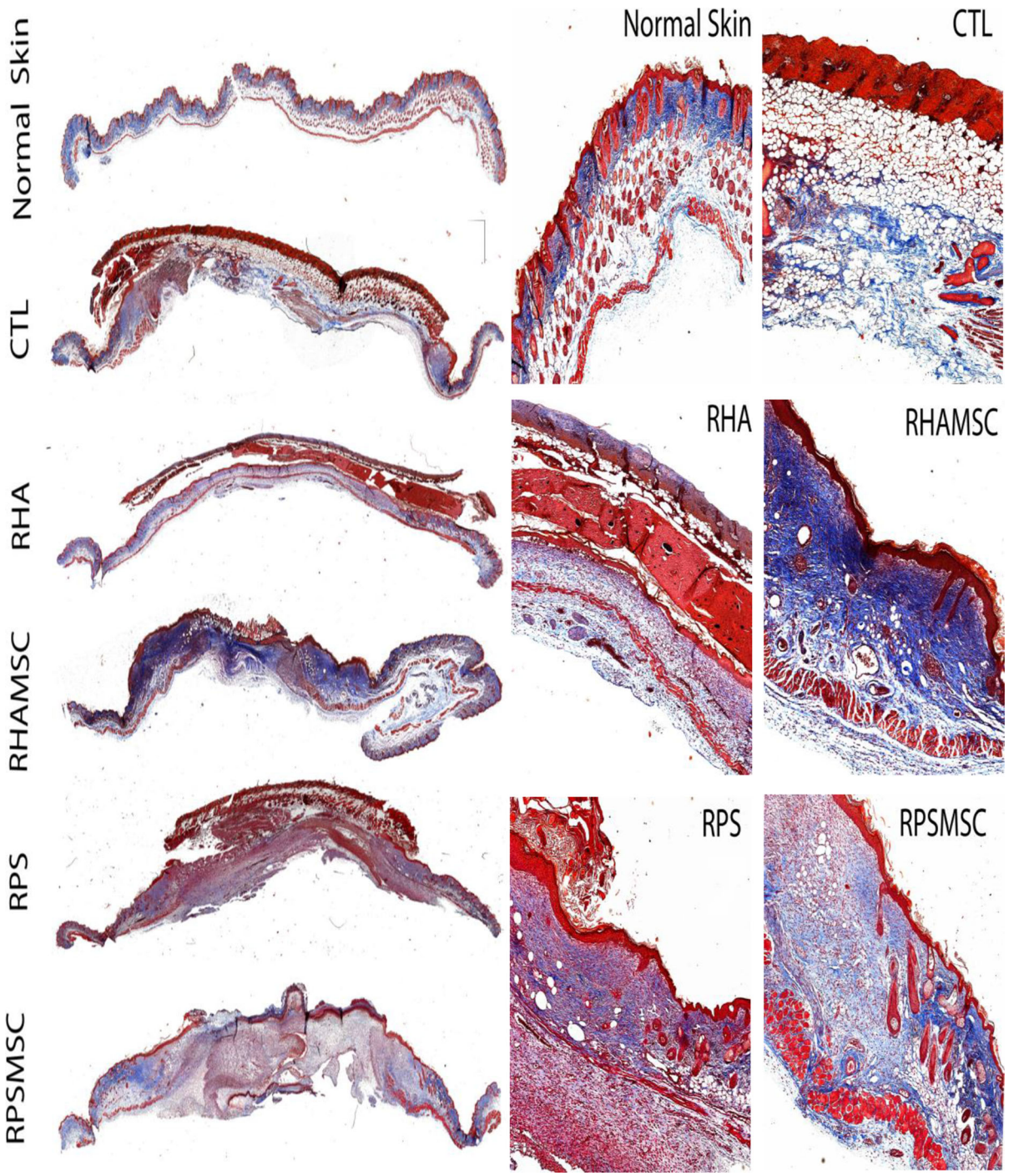

Fig. 6 Constructs increase collagen deposition in the wounds at post-treatment day 14. Masson stain at post-burn day 14. The images to the left are complete reconstructions of the tissues, whereas those to the right are enlarged images of the tissues. Scale bars represent 50 μm

Herovici staining was performed to determine whether the collagen deposited into the wounds was newly synthesized (mainly type III) or more mature (type I). As shown in non-wounded skin (Fig. 7), there

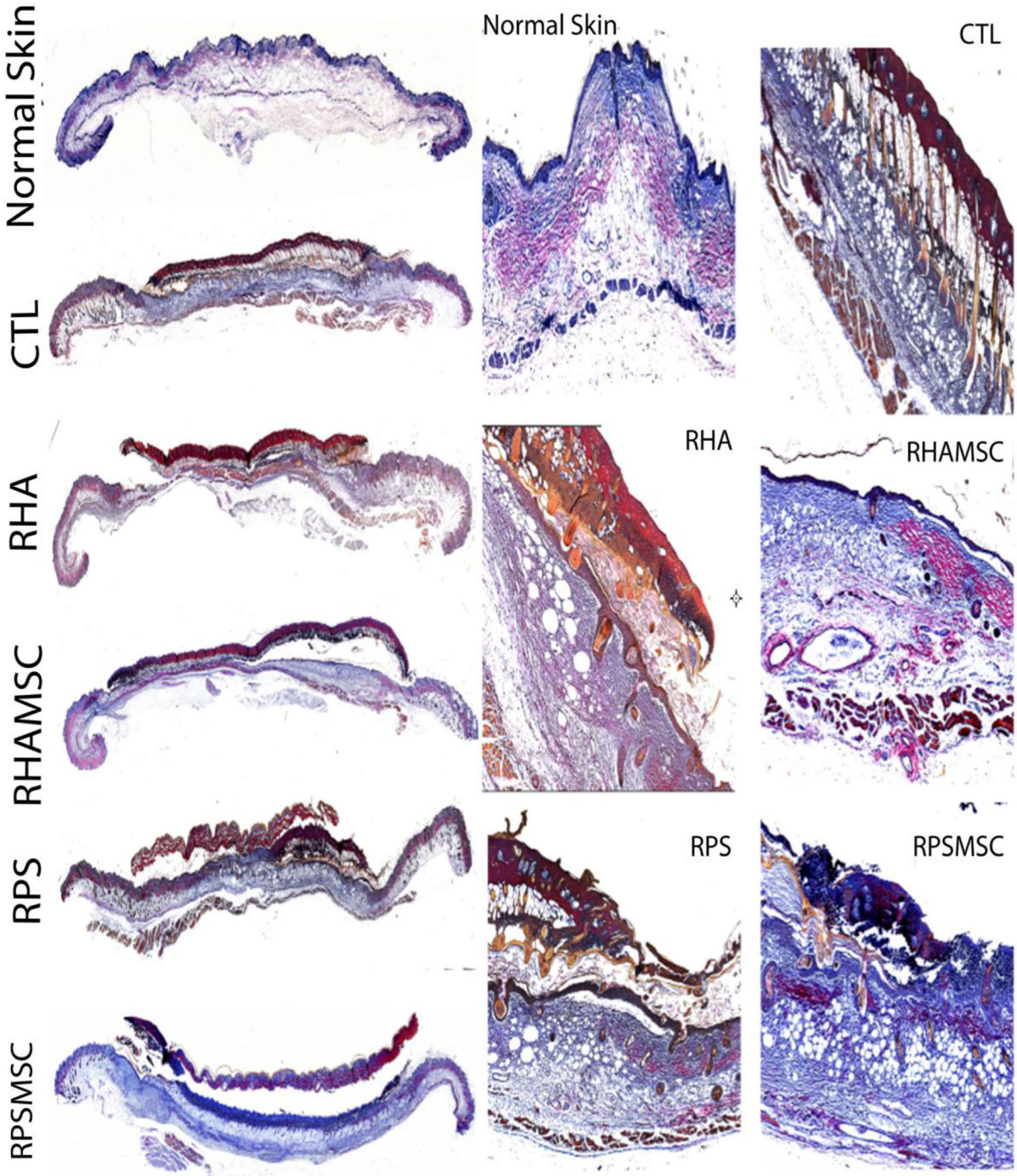

Fig. 7 Treatments with constructs enhance mature collagen deposition. Herovici stain at post-burn day 7. The images to the left are complete reconstructions of the tissues, whereas those to the right are enlarged images of the tissues. Scale bars represent 50 μm

is a specific separation between the two layers of the dermis. The papillary layer of the dermis shows newly synthesized collagen (stained in blue), whereas the reticular dermis expresses mature collagen (stained red). On day 7-post burn; wounds with conventional treatment only exhibited young collagen deposition in

the dermis, whereas the non-cellularized RHA and RPS treatments induced deposition of mature collagen. Deposition was enhanced by the addition of MSC, especially in the MSC-cellularized RHA construct on post-treatment day 7. By day 14-post treatment, re-epithelialization progress started in all treatments and there was a combination of newly synthesized and mature collagen composition in ECM. Remarkably MSC-cellularized constructs had an increased deposition of mature collagen (Fig. 8).

By day 7-post treatment, presence of Type I collagen was analyzed via immunofluorescence assay. This protein is abundant in the dermis of healthy skin; however, by day 7-post burn, collagen was absent in wounded tissue (control with petroleum jelly). Non-cellularized RHA and RPS showed an increase of type I collagen in their composition compared to petroleum jelly treatment; but the addition of MSC in both cases resulted in major detection of Type I collagen in early stages of wound healing (Figs. 9 and 10).

Discussion

Autologous skin graft is the gold standard coverage of third-degree burns. For patients who have suffered burns of greater than 40% TBSA, complications ensue and availability of healthy skin to perform autografts is limited. Tissue engineering allows manufacture of cellularized skin substitutes that can contain fibroblasts, keratinocytes, or both cell types cultured onto diverse synthetic or biological materials as an alternative skin coverage treatment for these patients. Radiosterilized human amnion (RHA) and radiosterilized pig skin (RPS) are two biocompatible materials that prevent water loss, infections and offer an extracellular matrix composition similar to human skin. Besides, they are widely available, and have a low cost. We treated deep burn wounds with RHA or RPS in combination with adipose-derived mesenchymal stromal cells to analyze the cellular process involved in wound healing progress.

Skin coverage with RHA decreases granulation tissue. This could be indicative of a decrease in inflammation, since it has been reported that amnion contains IL-10, which is an anti-inflammatory cytokine that has been related to regenerative process. This suggests a possible mechanism through which granulation tissue is reduced, but it needs be further analyzed (Genilhu Bomfim Pereira et al. 2015; King et al. 2014). By contrast, RPS enhances the granulation tissue. This response could be due to extracellular matrix proteins or the cells found in porcine skin; also explaining presence of B-lymphocytes and other immune cells, even when Nu/Nu mice were used in the study. Previous reports have shown that RPS induces release of interleukin-1β (Sánchez-Sánchez et al. 2015), which is capable of promoting proliferation of keratinocytes during re-epithelization phase.

However, skin coverage with adipose-derived mesenchymal cells seeded onto RPS reduces granulation tissue formation in wound site. It has been reported that MSC have immunomodulatory properties via IL-10 and IL-6 secretion (Kyurkchiev 2014). Growth factors and cytokines secretion profile could help us understand whether MSC have an active role during immune modulation. This release of growth factors could induce synthesis of collagen by resident dermal fibroblasts, or MSC could help synthesizing it by them. It is also possible that mesenchymal stromal cells could differentiate into fibroblasts and contribute to collagen deposition. All these questions need to be answered in the future.

MSC-cellularized wound coverage promoted type I collagen (COLI) deposition, which was more abundant by day 14 post-treatment, as revealed by Herovici staining and immunodetection. This suggests that there is a change in expression from type III collagen (COLIII) to type I in those mice treated with the cellularized scaffolds. This process could be explained as an acceleration of skin repair, since collagen synthesis improves from day 7 post-treatment compared to control group; however, they never reach type I collagen levels found in healthy skin (Figs. 9 and 10). At this stage, ECM synthesis was fast due to absence of re-epithelization. This could also explain formation of scars. Evaluating this process is not easy since mice repair deep wounds by contraction, they do not have the same mechanism as humans and they do not develop scars (Abdullahi et al. 2014; Domergue et al. 2015). This is considered a disadvantage because one of the major problems in human wound healing is scar development. Scars develop from a high inflammatory process that generates an imbalance between COLI and COLIII deposition, causing formation of keloid scars, predominantly constituted by COLI (Sidgwick and Bayat 2012).

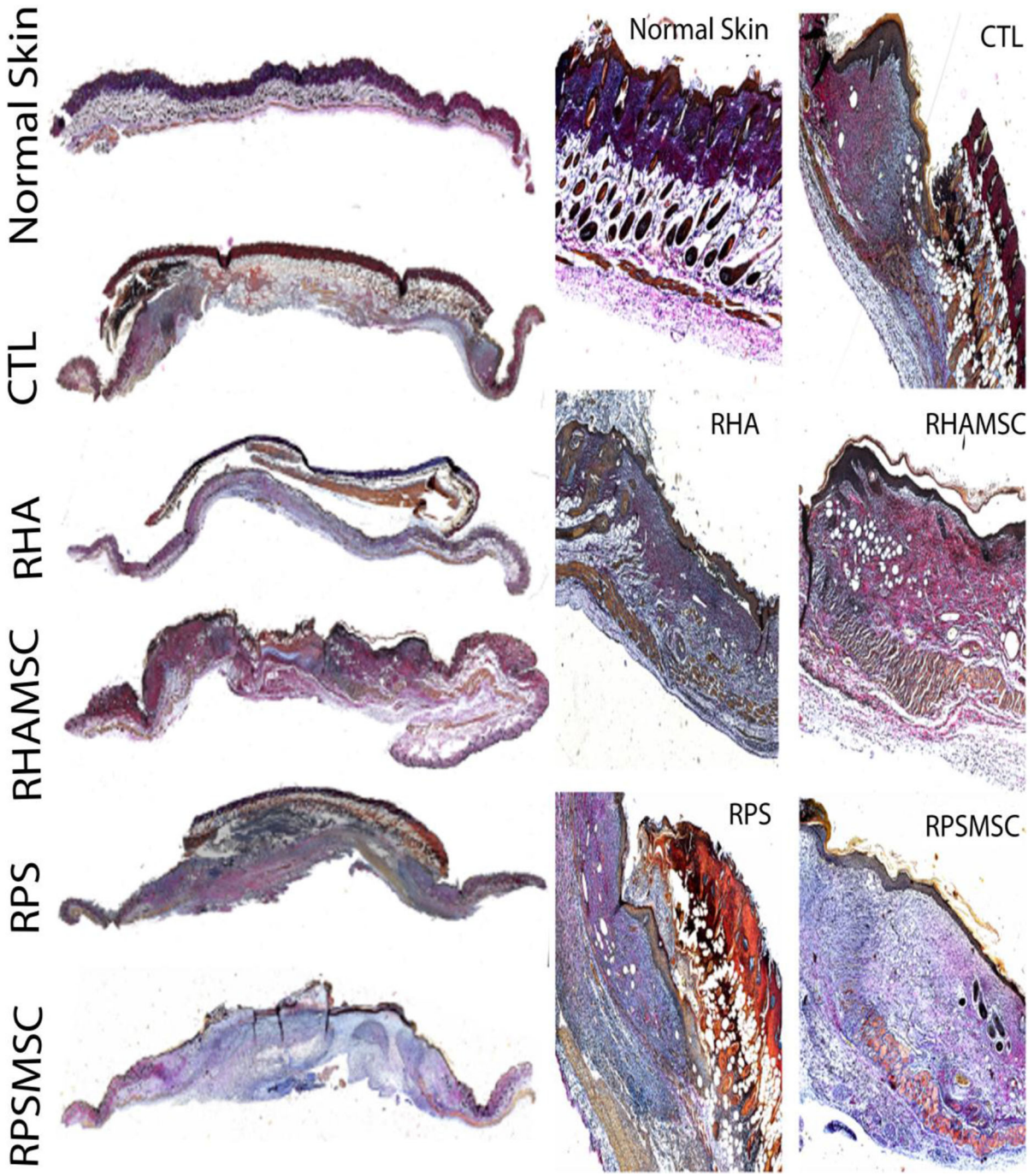

Fig. 8 RHA in combination with MSC promotes collagen maturation at post-burn day 14. Herovici stain at post-burn day 14. The images to the left are complete reconstructions of the tissues, whereas those to the right are enlarged images of the tissues. Scale bars represent 50 μm

Mice model does offer some advantages; it is cost-effective compared to bigger animals, there is no need for large areas to maintain them and they provide us with an approach for the cellular mechanisms involved in the wound healing process. Contraction as a mechanism mice have to heal wounds; as result, they

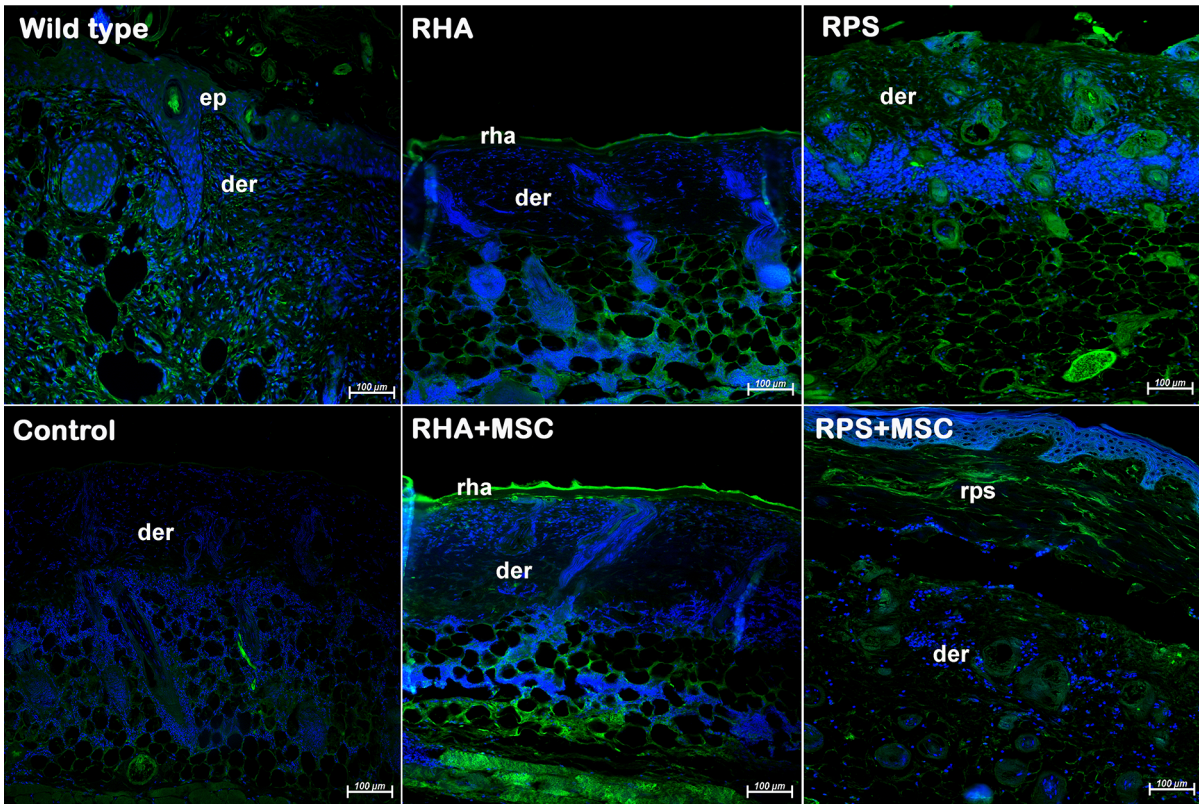

Fig. 9 Biomaterials and constructs show mild type I collagen at post-treatment day 7. Immunofluorescences to detect type I collagen (green) at post-treatment day 7. Nuclei are stained with DAPI (blue). Scale bars represent 100 µm

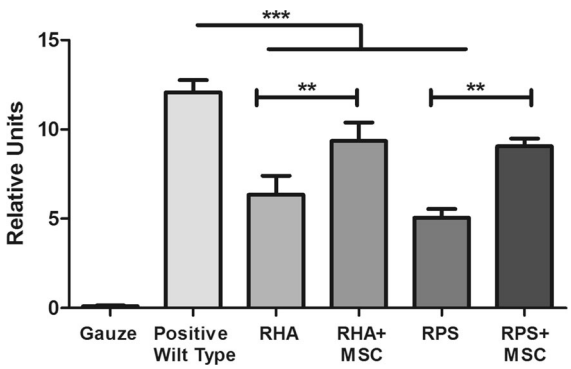

Fig. 10 Quantitation of type I collagen at post-treatment day 7. Graph shows the quantitation of type I collagen detected by immunofluorescence at treatment day 7. $^{***}p < 0.0001$, $^{**}p < 0.001$, ANOVA analysis and Tukey post-hoc test

heal deep wounds in a short time (Domergue et al. 2015). This could be the reason for no evident differences in wound closure between treatments versus controls, even when higher collagen deposition was observed in the animals treated with ASC-cellularized RHA and ASC-cellularized RPS.

Conclusions

This research provides evidence that radiosterilized human amnion and radiosterilized pigskin cellularized with adipose-derived mesenchymal stromal cells promote and increase collagen deposition during wound healing progress. These constructs have the potential to be further used as skin coverage for clinical treatment of burned patients. However, more studies are necessary to elucidate the role of MSC and their interaction with these biomaterials during wound healing.

Acknowledgements The authors express their gratitude to Dr. Javier PÉREZ GALLAGA and Dr. Elena CONTRERAS FIGUEROA for surgical procedures and animal care. BSc. Julieta GARCÍA-LÓPEZ for histological processing at Instituto Nacional de Rehabilitación Luis Guillermo Ibarra Ibarra. We

also acknowledge Daniel REBOYO BARRIOS for biomaterial processing at the *Banco de Tejidos Radioesterilizados del Instituto Nacional de Investigaciones Nucleares*.

Funding This work was supported by the Consejo Nacional de Ciencia y Tecnología, Project numbers 262103 and B-S-40505. It was also supported by the International Atomic Energy Agency through the IAEA Research Contract No. 18278 (2014–2019).

Data availability statement The datasets generated during and/or analysed during the current study are available from the corresponding author on reasonable request.

Declarations

Conflict of interest The authors declare that they have no conflict of interests.

References

Abdullahi A, Amini-Nik S, Jeschke MG (2014) Animal models in burn research. Cell Mol Life Sci 71:3241–3255

Aggarwal S, Pittenger MF (2005) Human mesenchymal stem cells modulate allogeneic immune cell responses. Blood 105:1815–1822. https://doi.org/10.1182/blood-2004-04-1559

Auger FA, Lacroix D, Germain L (2009) Skin substitutes and wound healing. Skin Pharmacol Physiol 22:94–102

Böttcher-Haberzeth S, Biedermann T, Reichmann E (2010) Tissue engineering of skin. Burns 36:450–460

Domergue S, Jorgensen C, Noël D (2015) Advances in research in animal models of burn-related hypertrophic scarring. J Burn Care Res 36:e259–e266. https://doi.org/10.1097/BCR.0000000000000167

Fathke C (2004) Contribution of bone marrow-derived cells to skin: collagen deposition and wound repair. Stem Cells 22:812–822. https://doi.org/10.1634/stemcells.22-5-812

Galipeau J, Sensébé L (2018) Mesenchymal stromal cells: clinical challenges and therapeutic opportunities. Cell Stem Cell 22:824–833

Genilhu Bomfim Pereira M, Alvaro Pereira Gomes J, Vicente Rizzo L, et al (2015) Cytokine dosage in fresh and preserved human amniotic membrane

Hocking AM, Gibran NS (2010) Mesenchymal stem cells: paracrine signaling and differentiation during cutaneous wound repair. Exp Cell Res 316:2213–2219

Jones I, Currie L, Martin R (2002) A guide to biological skin substitutes. Br J Plast Surg 55:185–193

King A, Balaji S, Le LD et al. (2014) Regenerative Wound Healing: The Role of Interleukin-10. https://doi.org/10.1089/wound.2013.0461

Kinsner A, Lesiak-Cyganowska E, Śladowski D (2001) In vitro reconstruction of full thickness human skin on a coposite collagen material. Cell Tissue Bank 2:165–171. https://doi.org/10.1023/A:1020196504392

Kyurkchiev D (2014) Secretion of immunoregulatory cytokines by mesenchymal stem cells. World J Stem Cells 6:552. https://doi.org/10.4252/wjsc.v6.i5.552

Llames S, García E, García V et al (2006) Clinical results of an autologous engineered skin. Cell Tissue Bank 7:47–53. https://doi.org/10.1007/s10561-004-7253-4

Martínez-Pardo ME, Mariano-Magaña D (2007) The tissue bank at the Instituto Nacional de Investigaciones Nucleares: ISO 9001:2000 certification of its quality management system. Cell Tissue Bank 8:221–231. https://doi.org/10.1007/s10561-006-9031-y

Peck MD (2011) Epidemiology of burns throughout the world. Part I: distribution and risk factors. Burns 37:1087–1100

Sánchez-Sánchez R, Brena-Molina A, Martínez-Lónez V et al (2015) Generation of two biological wound dressings as a potential delivery system of human adipose-derived mesenchymal stem cells. ASAIO J 61:718–725. https://doi.org/10.1097/MAT.0000000000000277

Sasaki M, Abe R, Fujita Y et al (2008) Mesenchymal stem cells are recruited into wounded skin and contribute to wound repair by transdifferentiation into multiple skin cell type. J Immunol 180:2581–2587. https://doi.org/10.4049/jimmunol.180.4.2581

Sidgwick GP, Bayat A (2012) Extracellular matrix molecules implicated in hypertrophic and keloid scarring. J Eur Acad Dermatology Venereol 26:141–152

Wu Y, Chen L, Scott PG, Tredget EE (2007) Mesenchymal stem cells enhance wound healing through differentiation and angiogenesis. Stem Cells 25:2648–2659. https://doi.org/10.1634/stemcells.2007-0226

Yildirimer L, Thanh NTK, Seifalian AM (2012) Skin regeneration scaffolds: a multimodal bottom-up approach. Trends Biotechnol 30:638–648